Electronic Supplementary Information

Photochemical Hydrogen Evolution from Water by a 1D-Network of Octahedral Ni_6L_8 Cages

Kilaparthi Sravan Kumar,[a‡] Vishwanath S. Mane,[c‡] Ashok Yadav,[a] Avinash S. Kumbhar,[c*] and Ramamoorthy Boomishankar*[ab]

[a] Department of Chemistry and [b] Centre for Energy Science, Indian Institute of Science Education and Research (IISER), Pune, Dr. Homi Bhabha Road, Pune – 411008, India

[c] Department of Chemistry, Savitribai Phule Pune University, Pune, 411007, India

*Corresponding authors E-mail: boomi@iiserpune.ac.in ; askum@chem.unipune.ac.in

‡Authors have equally contributed

Contents

Experimental Section

Materials and methods. All chemicals used for synthesis were purchased from Sigma-Aldrich and used as received without any further purification. TLC analysis was done on aluminium plates with silica gel 60 F254; Column chromatography was done on 200-300 mesh silica gel. 1H NMR spectra were recorded on Bruker Advanced 400 MHz DPX spectrometer using 1,1,1,1-tetramethyl silane (TMS) as an internal standard. Water was deionized using Millipore synergy system (18.2 MΩ cm resistivities) and was stored under argon atmosphere. UV-Visible absorption measurements were carried out in Shimadzu UV-2600 spectrophotometer. Thermogravimetric analysis (TGA) analysis was obtained from Perkin-Elmer STA 1000 instrument. The powder X-ray diffraction (PXRD) data were obtained from a Bruker-D8 Advance diffractometer. Dynamic light scattering (DLS) was performed using Nano ZS-90 setup (Malvern instruments).

Synthesis of 1. The ligand L was prepared using our previously reported procedure.1 To the stirred methanolic solution of L (10mg, 36mmol), a methanolic solution of $NiCl_2.6H_2O$ (6.41mg, 27mmol) was added dropwise at room temperature. The resultant solution was kept for slow evaporation and blue coloured crystals of 1 were obtained after one week (scheme 1). FTIR data in solid sample (cm^{-1}): 3370, 1633, 1588, 1473, 1398, 1355, 1261, 1230, 1197, 1131, 1052, 791, 745, 703, 642, 497, 433.

Scheme S1. Synthesis protocol of **1**

Photochemical Hydrogen generation. The visible-light-driven H_2 production experiments were performed in a 33 mL round-bottomed flask. In a typical experiment, the flask was filled with 5 mL of water solution containing 0.5mM $[Ru(byp)_3]^{+2}$, 0.3 M ascorbic acid as electron donor in pH 4 ascorbate buffer and 100-200 μM catalyst. The reaction flask was sealed with a rubber septum, carefully deaerated, and filled with nitrogen. The reaction samples were irradiated by a light-emitting diode (LED) light source (λ = 469 nm) at room temperature with equipped with a stir bar. The flask was connected to a pressure transducer (PXM409-002BAUSBH) was kept under temperature controlled water jacketed jar (25 ˚C). The evolved hydrogen gas was monitored by recording the increase in headspace pressure in every 10 s for 69 hours. The obtained pressure values were used in calculating number of moles of hydrogen evolved using the equation PV=nRT. The qualitative confirmation of evolved gas was performed by using Gas Chromatography (GC) Shimadzu GC 2014 (PORAPAK Q, length 2.0 m, ID 3.13 mm) with TCD detector. Control experiment were performed under the same conditions in the absence of catalyst. The thermodynamic and kinetic stabilities of 1 were measured using turnover number (TON) = [generated H_2]/[catalyst] in moles and turnover frequency (TOF) = TON/unit time, respectively.

Electrochemical experiments. Cyclic voltammetry (CV) experiments were conducted on a CH-electrochemical analyzer, Model 1100A using a three-electrode single-compartment cell including a glassy carbon working electrode, a Pt wire auxiliary electrode, and a SCE (Saturated calomel electrode) as a reference electrode. For all measurements, samples were degassed by bubbling nitrogen through the solution for 10 min. Tetrabutylammonium hexafluorophosphate and KNO_3 were used as the supporting electrolyte (0.1 M). The acetonitrile solvent and B. R. Buffer (Briton Robinson Buffer) were used as non-aqueous and aqueous solutions, respectively, for electrochemical studies.

Acetic acid was used as a proton source in acid dependent cyclic voltammetry experiment at 100 mV/s and Ag/AgCl as reference electrode.

Crystallography: Reflections were collected on a Bruker Smart Apex Duo diffractometer at 100 K using Mo Kα radiation (λ = 0.71073 Å). Structures were refined by full-matrix least squares against F2 using all data (SHELX).[2] Crystallographic data for all of these compounds are given in Tables S1 and S2 in the Supporting Information. All non-hydrogen atoms were refined anisotropically if not stated otherwise. Hydrogen atoms were constrained in geometric positions to their parent atoms. One of the chloride ion sites (Cl5) bound to the Ni3 atom is partially occupied and disordered with a coordinated water molecule (O1w). The unbound chloride ion (Cl6) is disordered over two sites and hence was refined freely with similar U-restraints. The H atoms of various water molecules were not located, but allowance has been made for them in the Formula and Formula weight entries in Table S1.

Crystallographic data: tables and figures

Table S1. Crystal data of **1**

Compound	**1**
Chemical formula	$C_{128}H_{156}Cl_{12}N_{24}Ni_6O_{24}Si_8$
Formula weight	3417.14
Temperature	100(2) K
Crystal system	Tetragonal
Space group	P4/n
a (Å); α (°)	22.724(8); 90°
b (Å); β(°)	22.724(8); 90°
c (Å); γ (°)	16.435(7); 90°
V (Å^3); Z	8487(7); 2
ρ (calc.) g cm^{-3}	1.337
μ(Mo Kα) mm^{-1}	0.963
2θmax (°)	25.024
R(int)	0.1813
Completeness to θ	99.5 %
Data / param.	7463/458
GOF	1.033
R1 [F>4σ(F)]	0.0880
wR2 (all data)	0.2959
max. peak/hole (e.Å^{-3})	1.618/-0.929

Table S2. Selective Bond length and bond angle of **1**

Compound	Bond length (Å)		Bond angle	
1	Ni(1)-N(13)	2.087(6)	N(13)-Ni(1)-N(13)#1	178.6(4)
	Ni(1)-N(13)#1	2.087(6)	N(13)-Ni(1)-N(13)#2	89.990(7)
	Ni(1)-N(13)#2	2.087(6)	N(13)#1-Ni(1)-N(13)#2	89.992(5)
	Ni(1)-N(13)#3	2.087(6)	N(13)-Ni(1)-N(13)#3	89.993(5)
	Ni(1)-Cl(1)	2.362(6)	N(13)#1-Ni(1)-N(13)#3	89.992(7)
	Ni(1)-Cl(2)#4	2.583(4)	N(13)#2-Ni(1)-N(13)#3	178.6(4)
	Ni(2)-N(43)	2.120(7)	N(13)-Ni(1)-Cl(1)	90.69(18)
	Ni(2)-N(43)#1	2.120(7)	N(13)#1-Ni(1)-Cl(1)	90.69(18)
	Ni(2)-N(43)#2	2.120(7)	N(13)#2-Ni(1)-Cl(1)	90.69(18)
	Ni(2)-N(43)#3	2.120(7)	N(13)#3-Ni(1)-Cl(1)	90.69(18)
	Ni(2)-Cl(3)	2.340(6)	N(13)-Ni(1)-Cl(2)#4	89.31(18)
	Ni(2)-Cl(2)	2.525(4)	N(13)#1-Ni(1)-Cl(2)#4	89.31(18)
	Ni(3)-N(63)	2.104(8)	N(13)#2-Ni(1)-Cl(2)#4	89.31(18)
	Ni(3)-N(53)#2	2.107(7)	N(13)#3-Ni(1)-Cl(2)#4	89.31(18)
	Ni(3)-N(23)#2	2.113(8)	Cl(1)-Ni(1)-Cl(2)#4	180.0
	Ni(3)-N(33)	2.114(8)	N(43)-Ni(2)-N(43)#1	179.7(4)
	Ni(3)-O(1W)	2.170(18)	N(43)-Ni(2)-N(43)#2	90.000(2)
	Ni(3)-Cl(4)	2.334(3)	N(43)#1-Ni(2)-N(43)#2	90.000(2)
	Ni(3)-Cl(5)	2.450(6)	N(43)-Ni(2)-N(43)#3	89.999(2)
	Cl(2)-Ni(1)#5	2.583(4)	N(43)#1-Ni(2)-N(43)#3	90.000(2)
	Cl(6)-Cl(6')	0.704(9)	N(43)#2-Ni(2)-N(43)#3	179.7(4)
	Si(1)-C(11)	1.853(9)	N(43)-Ni(2)-Cl(3)	90.17(18)
	Si(1)-C(21)	1.874(10)	N(43)#1-Ni(2)-Cl(3)	90.17(18)
	Si(1)-C(1)	1.876(9)	N(43)#2-Ni(2)-Cl(3)	90.17(18)
	Si(1)-C(31)	1.881(10)	N(43)#3-Ni(2)-Cl(3)	90.17(18)
	Si(2)-C(51)	1.854(10)	N(43)-Ni(2)-Cl(2)	89.83(18)
	Si(2)-C(61)	1.856(10)	N(43)#1-Ni(2)-Cl(2)	89.83(18)
	Si(2)-C(2)	1.857(9)	N(43)#2-Ni(2)-Cl(2)	89.83(18)
	Si(2)-C(41)	1.874(9)	N(43)#3-Ni(2)-Cl(2)	89.83(18)
	C(1)-H(1A)	0.9800	Cl(3)-Ni(2)-Cl(2)	180.0
	C(1)-H(1B)	0.9800	N(63)-Ni(3)-N(53)#2	89.4(3)
	C(1)-H(1C)	0.9800	N(63)-Ni(3)-N(23)#2	179.4(3)
	C(2)-H(2A)	0.9800	N(53)#2-Ni(3)-N(23)#2	90.0(3)

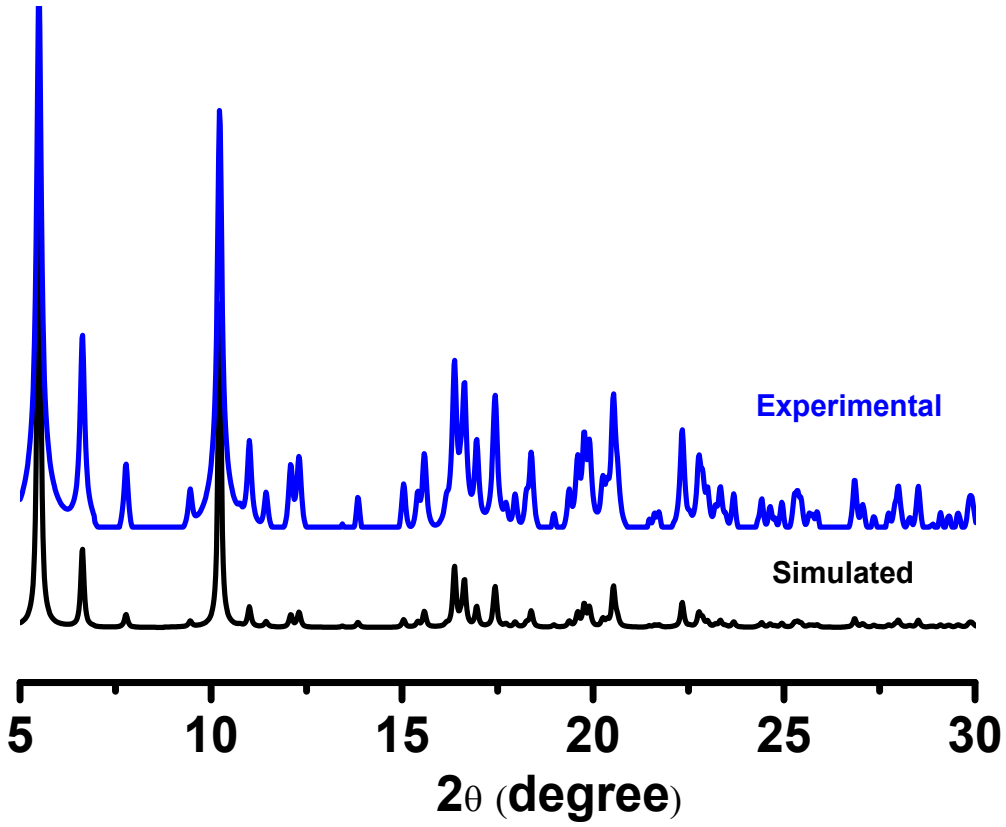

Figure S1. Experimental X-ray powder diffraction patterns of **1** (Blue) and the simulated (Black) patterns obtained from the single crystal X-ray diffraction analysis.

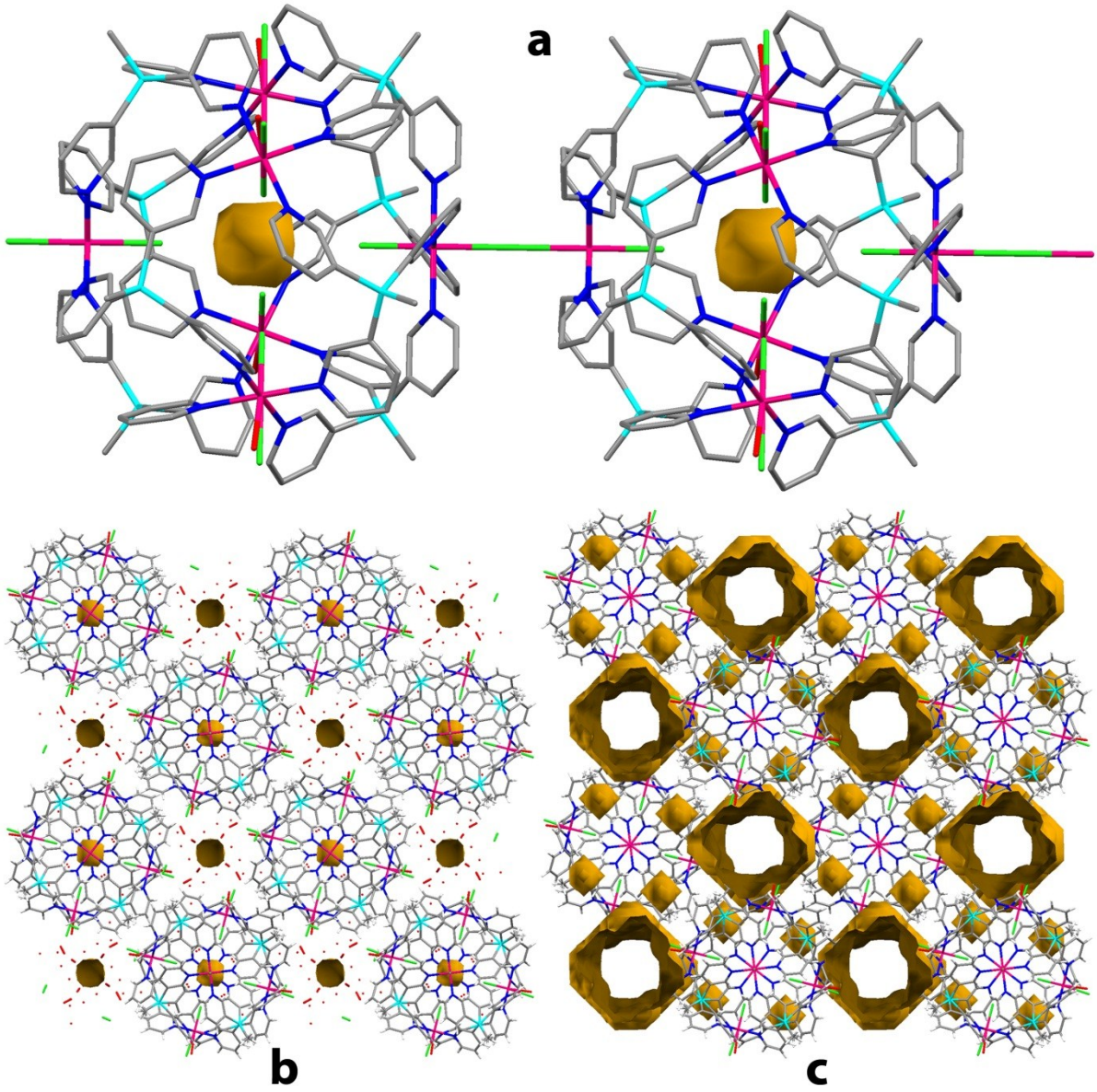

Figure S2. View of the intrisinc and extrinsic void surfaces of **1**. (a) Contact surface view of the intrinsic cage cavities in **1**. (b) Packing diagram of **1** showing the location of the solvated and unbound chloride ions in **1** and (c) view of the solvent accessible viods present in the extrinsic channels present in the crystal packing of **1**; solvated water molecules have been omitted for clarity.

Spectral and thermal data

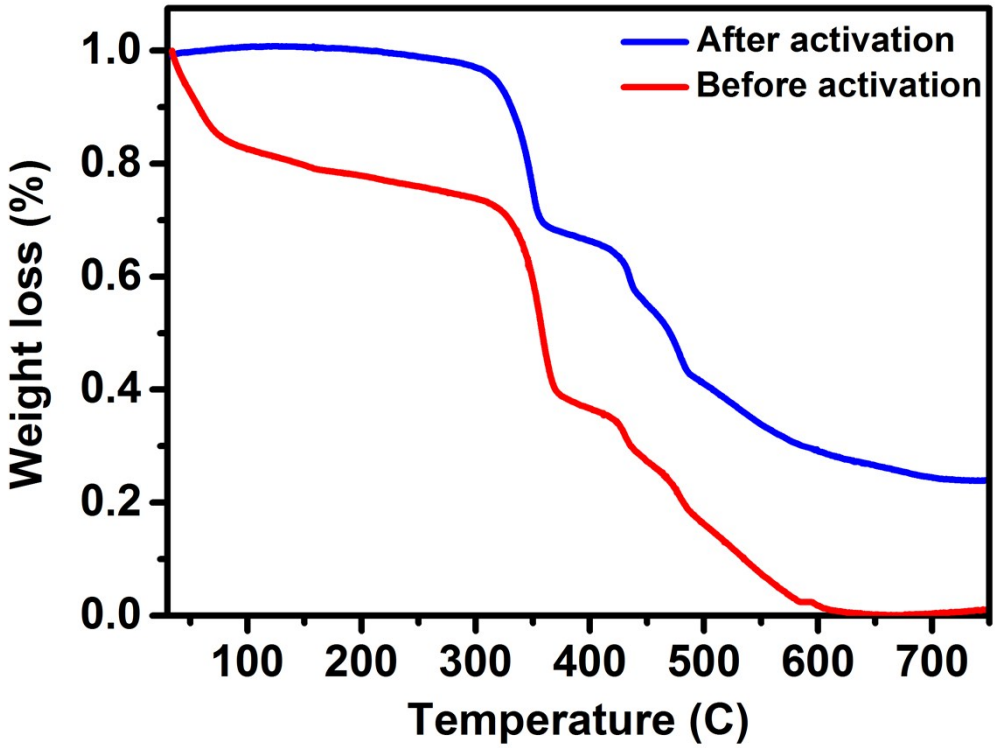

Figure S3. Thermogravimetric analysis of **1** before (red) and after (blue) activation

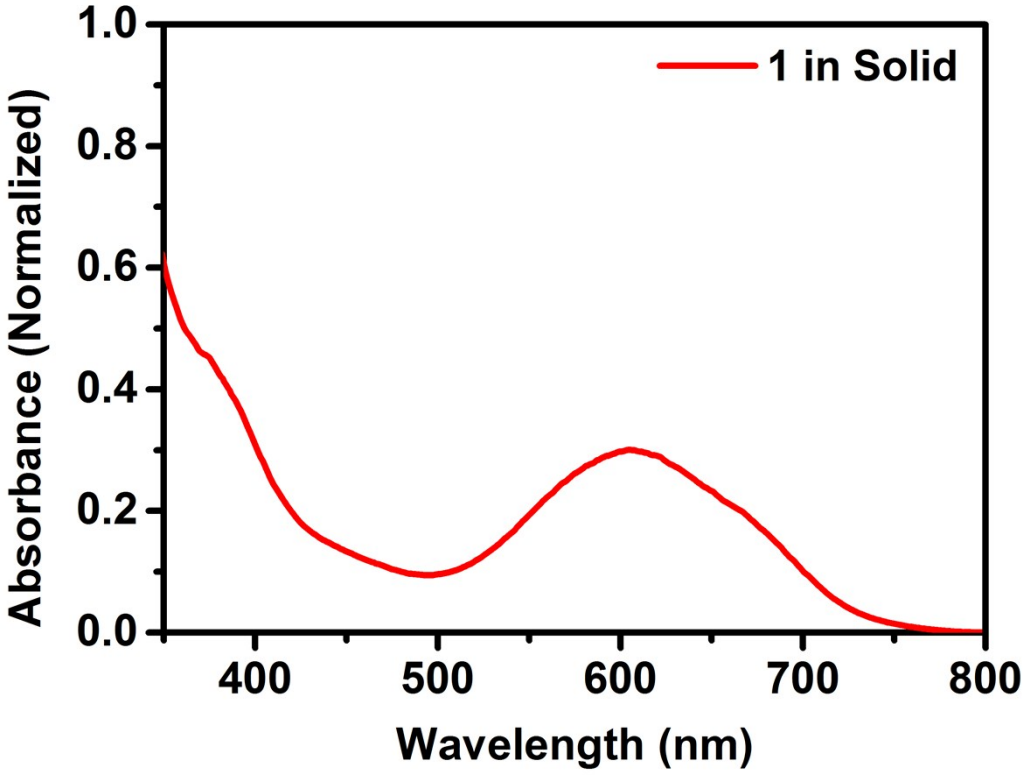

Figure S4. UV-Visible spectrum of **1** in the solid state.

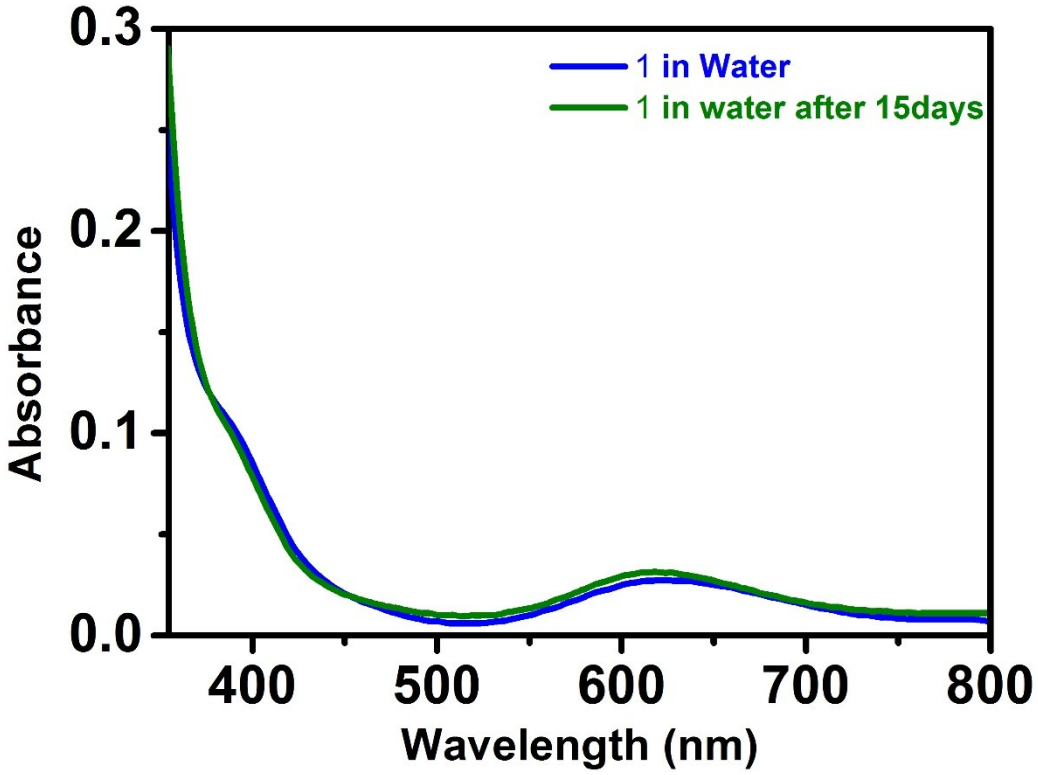

Figure S5. UV-Visible spectra of **1** in water: Spectra of the as made solution (Blue) and after 15 days (green)

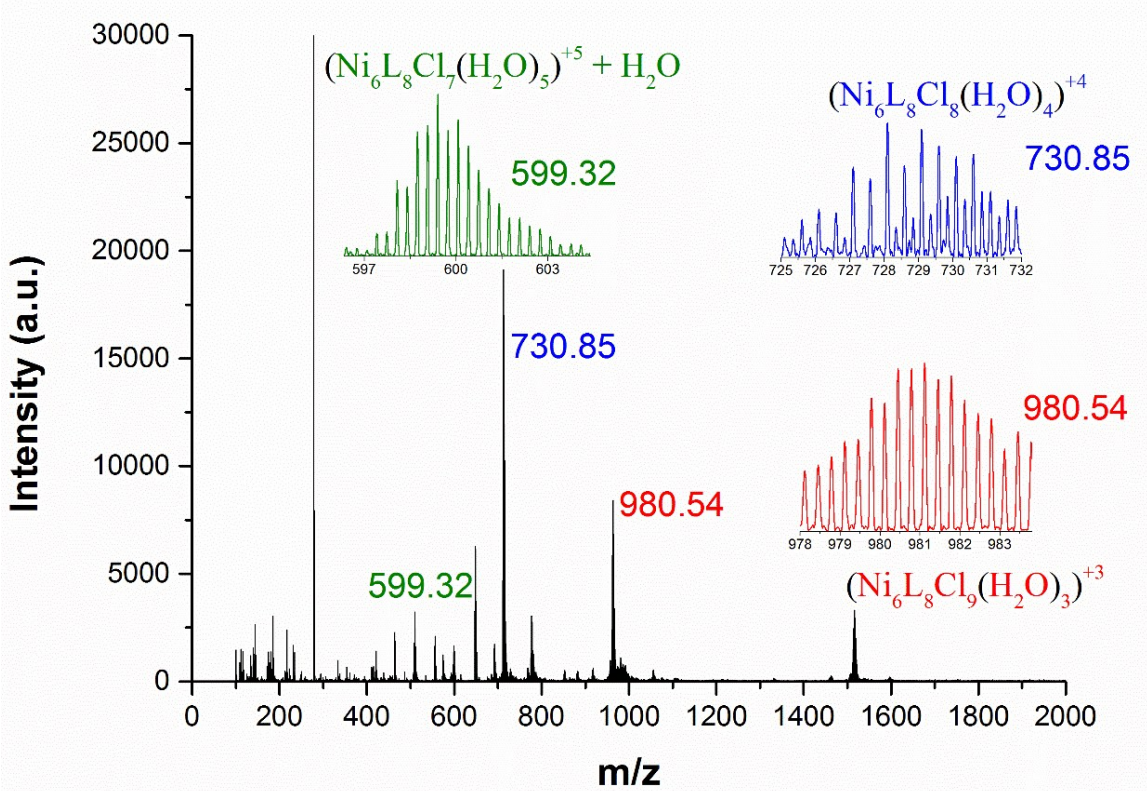

Figure S6. Electrospray ionization (ESI) mass spectra of **1**

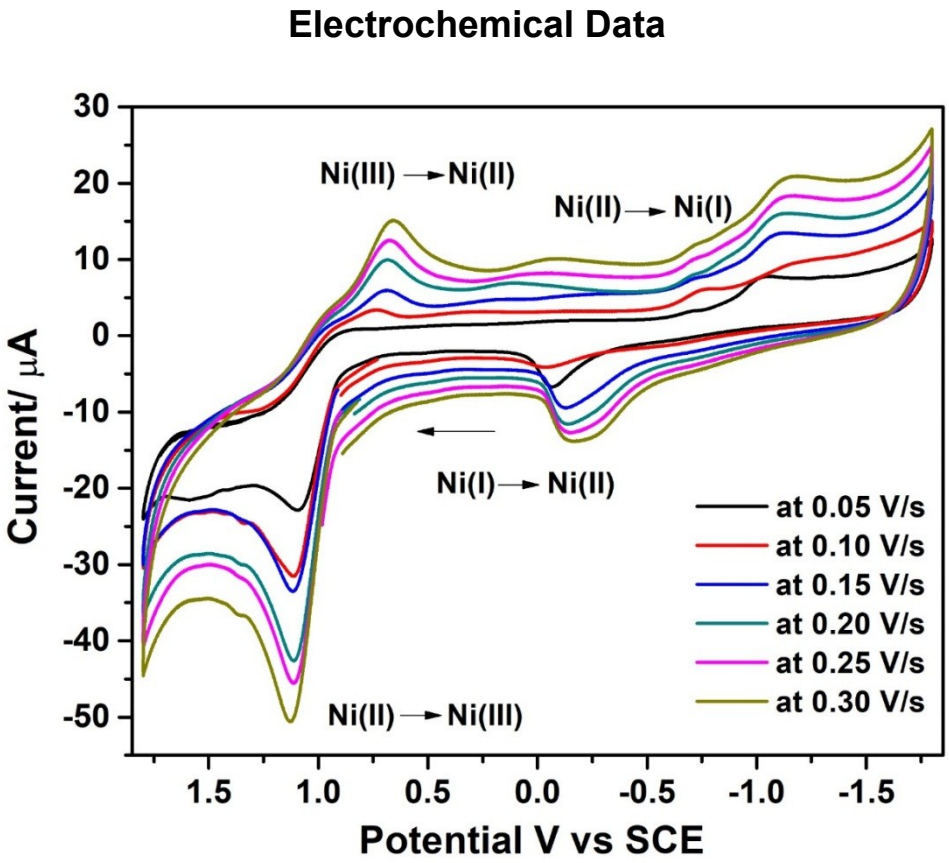

Figure S7. Scan rate dependent cyclic voltammetry of **1** in acetonitrile solution

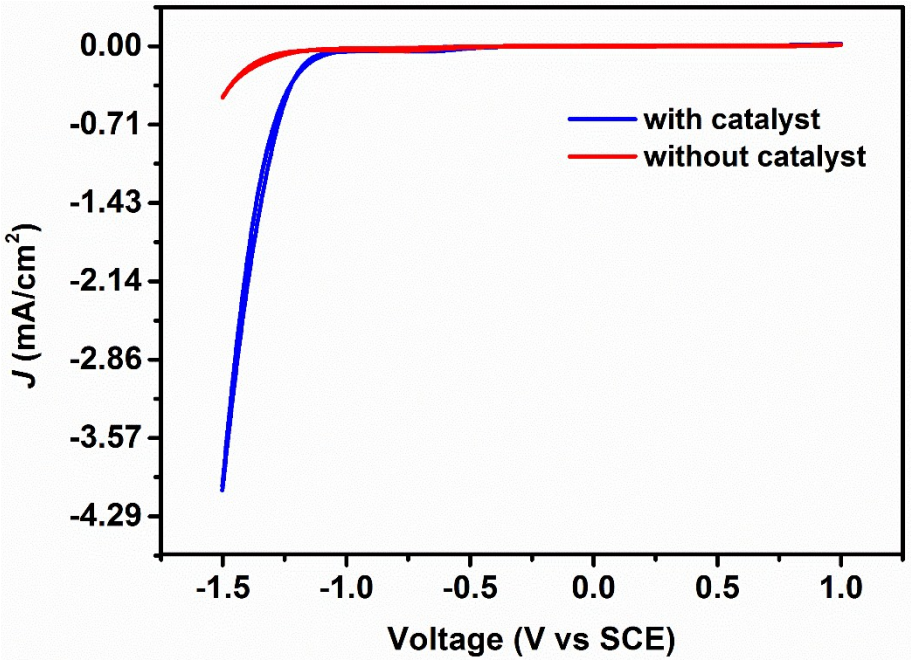

Figure S8. Cyclic voltammetry of the BR buffer solution at pH 4 in the presence and absence of **1**

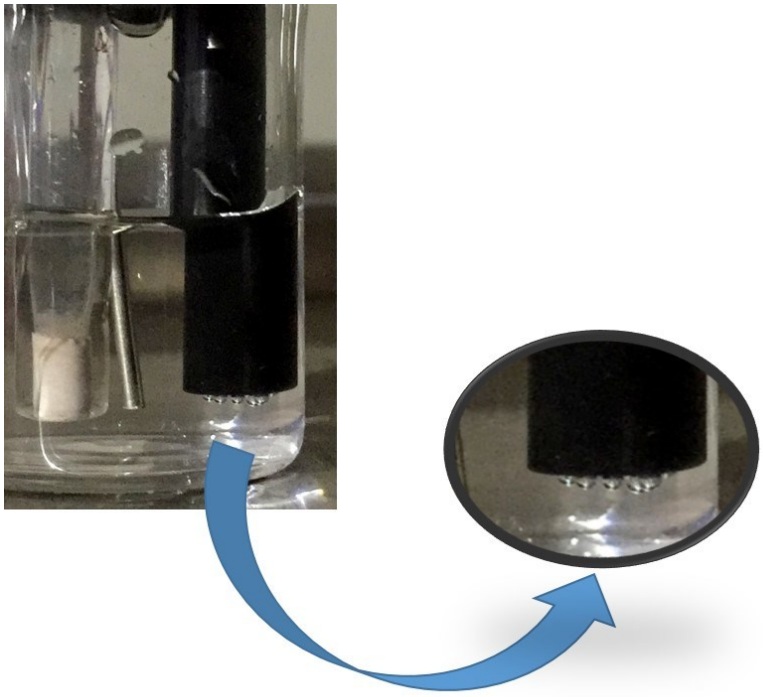

Figure S9. Evolution of hydrogen gas at working electrodes in reaction cell

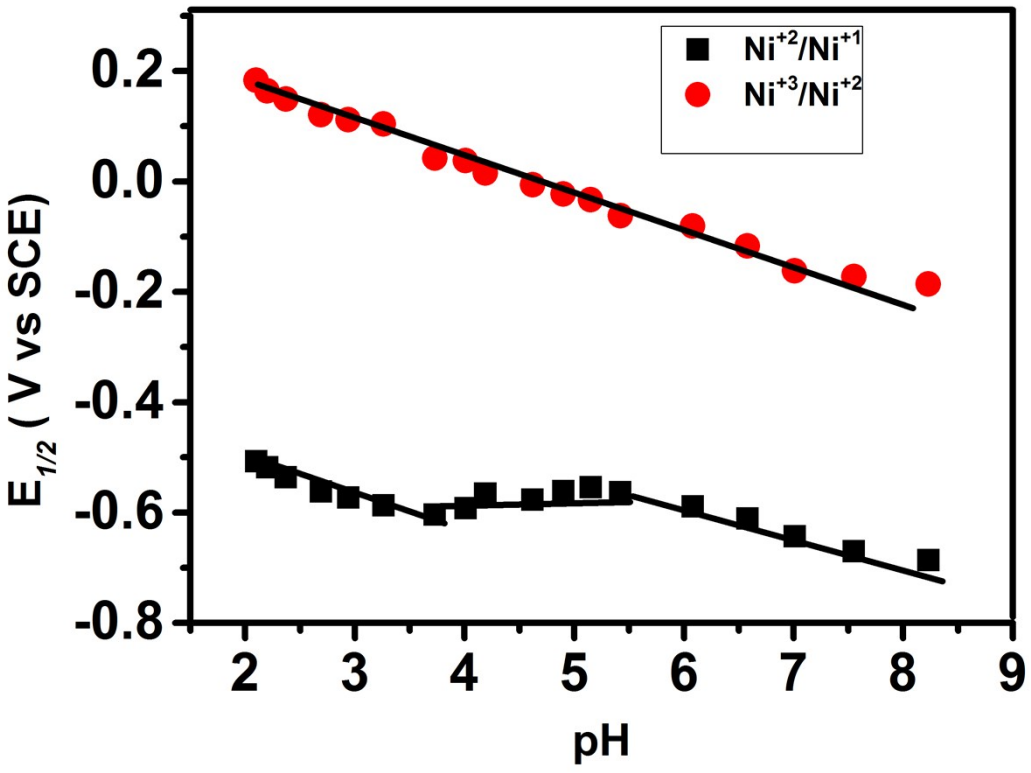

Figure S10. Pourbaix diagram of **1** in BR buffer solution using differential pulse voltammetry

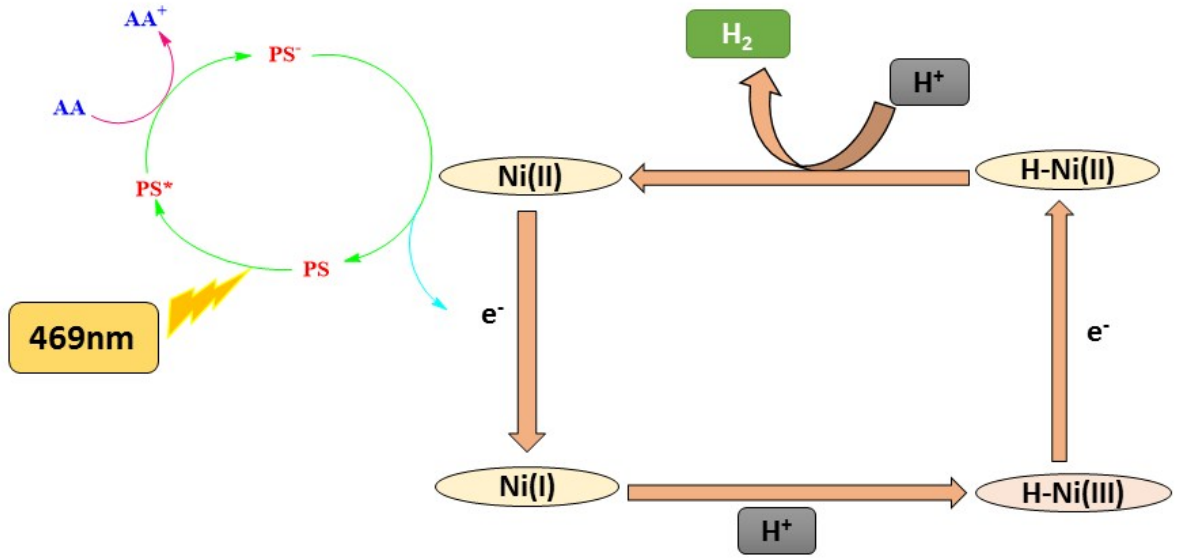

Figure S11. Probable mechanism for hydrogen evolution reaction using **1** as catalyst.

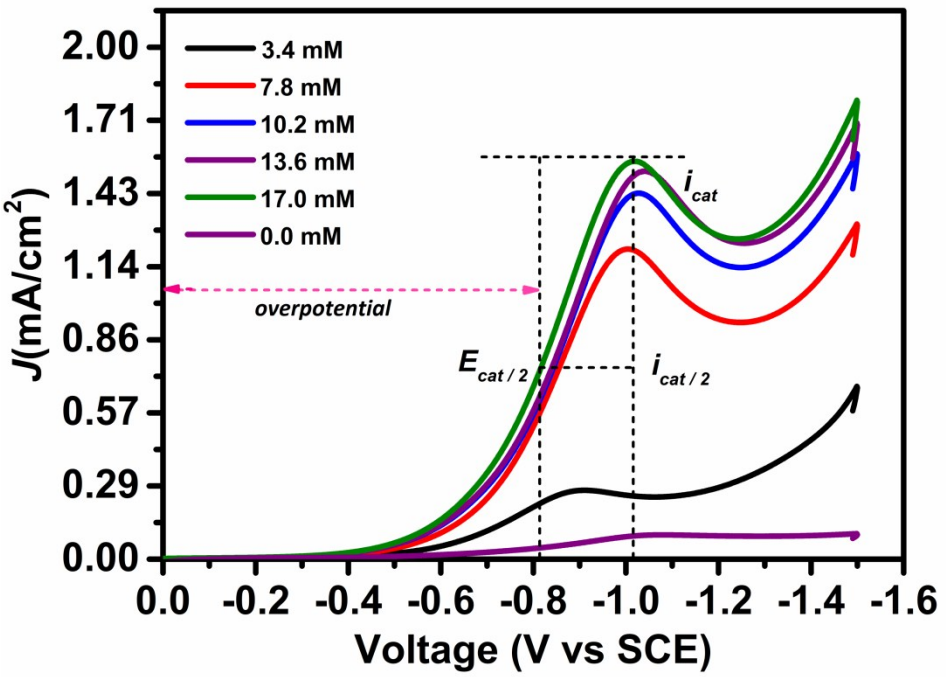

Figure S12. Cyclic Voltammetry of **1** by varying concentrations of acetic acid in acetonitrile at room temperature

[3]Overpotential = [$E_{cat/2}$ - $E_{HA/H2}$]

$E_{cat/2}$ = half catalytic potential, i_{cat} = catalytic current

$E_{HA/H2}$ = reduction potential of AA, $i_{cat/2}$ = catalytic current at $E_{cat/2}$

pKa and $E_{HA}/_{H2}$ for Acetic Acid in acetonitrile are 22.3 and -1.46 V vs Fc^{+}/Fc respectively.[4]

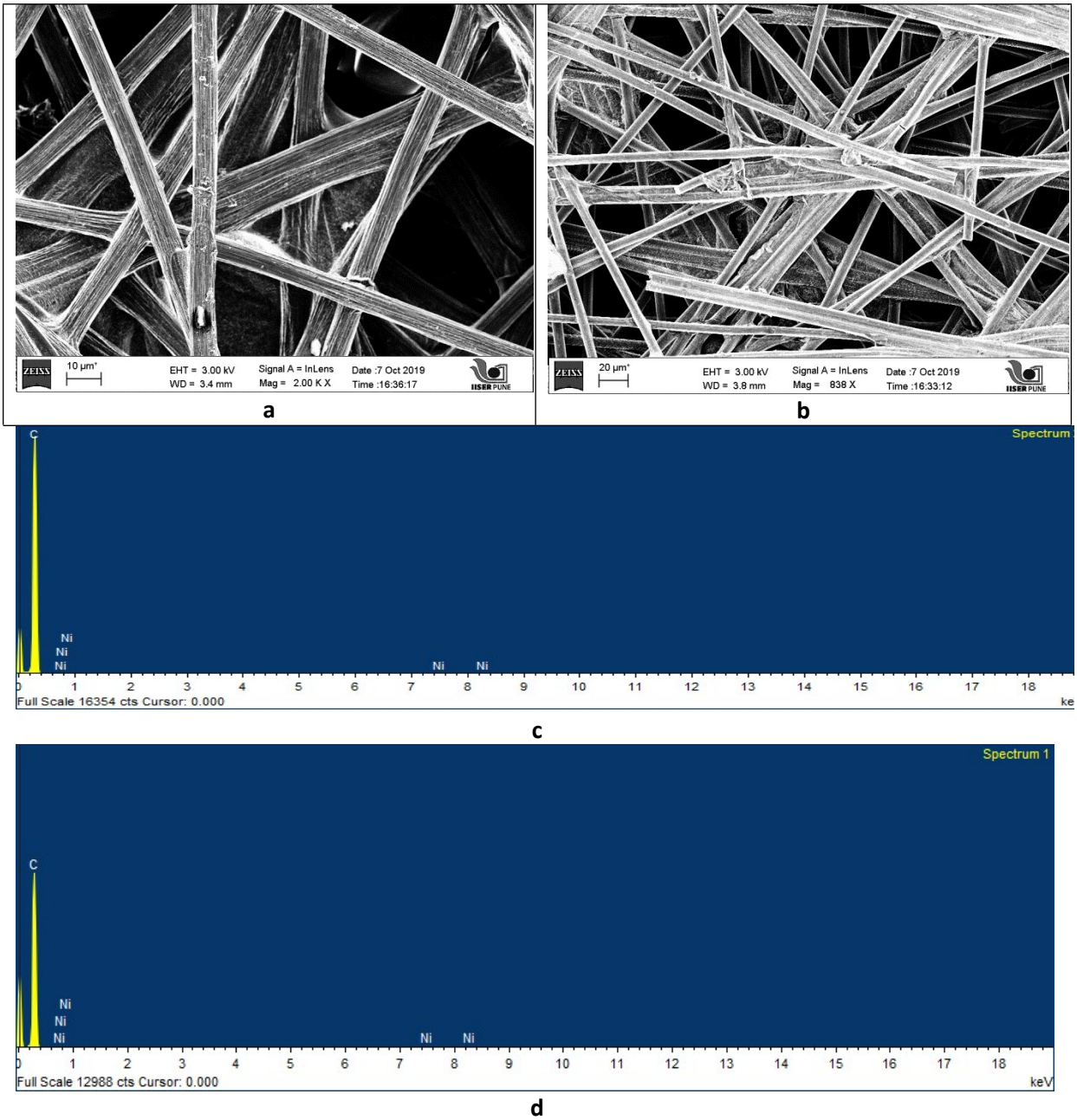

Figure S13. (a) FESEM of carbon electrode before electrolysis in BR buffer solution. (b) SEM of carbon electrode after electrolysis in BR buffer solution. (c) EDX of carbon electrode before electrolysis in BR buffer solution. (d) EDX of carbon electrode after electrolysis in BR buffer solution.

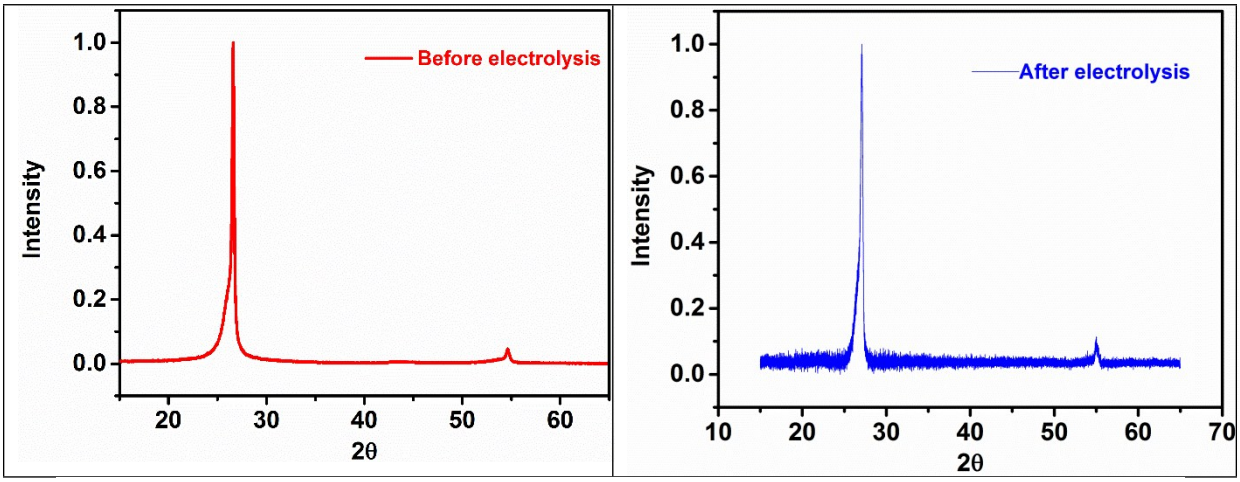

Figure S14. (a) PXRD profiles of the carbon electrode before and after electrolysis in 0.03M BR buffer solution.

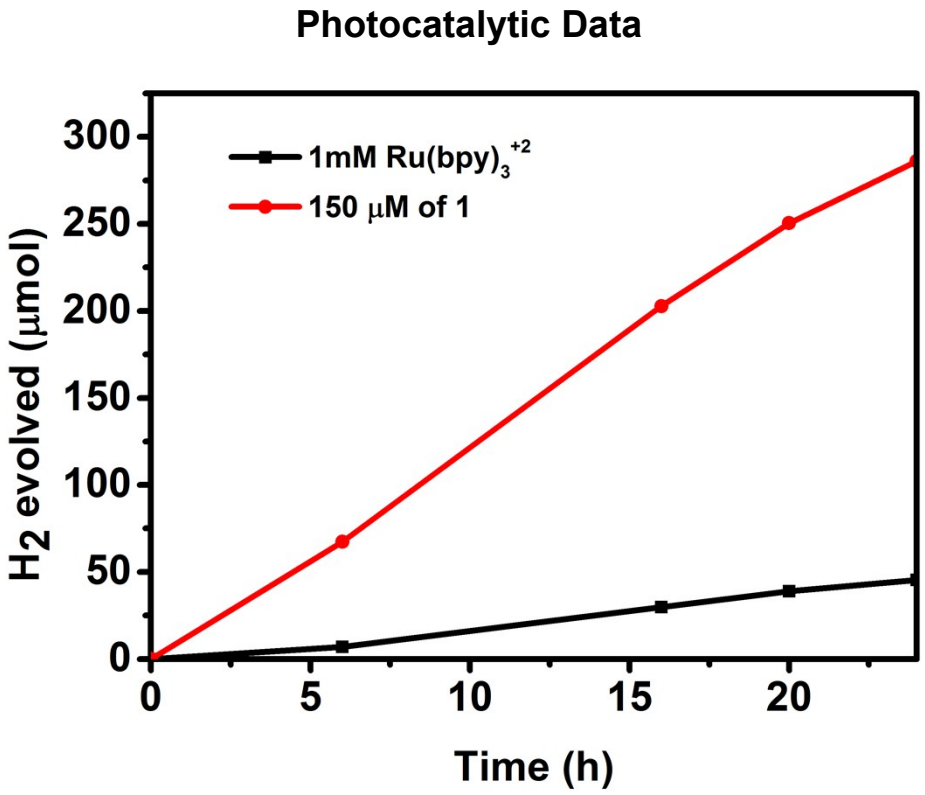

Figure S15. Controlled photocatalytic experiment using 1mM $Ru(bpy)_3^{+2}$ as both catalyst and photosensitizer and ascorbic acid as sacrificial electron donor and its comparison with the reaction catalyzed by 150 μM of **1**.

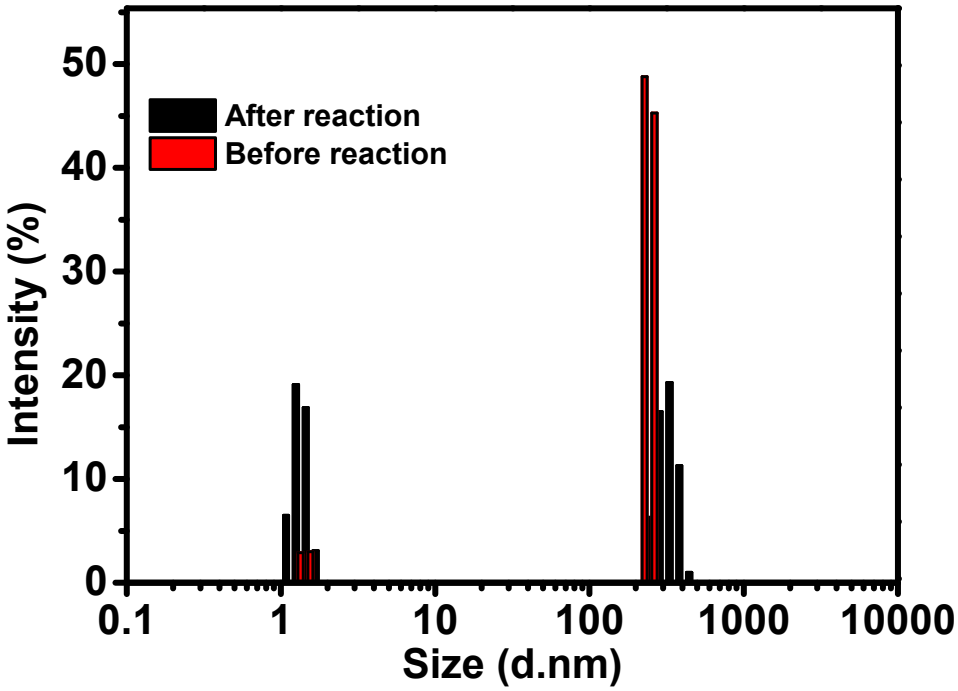

Figure S16. DLS analysis before and after photocatalytic reaction.

Table S3. Photocatalytic HER activity of **1** at various concentrations

Catalyst Concentration (μM)	Turnover number (TON)	Turnover frequency (TOF) (h^{-1})
25	2824	41.0
50	1895	27.5
100	1213	17.6
150	870	12.6
200	682	9.9

Comparative Tables for Electro- Photocatalytic Reactions

Table S4. Comparative electrocatalytic HER activity of Ni(II) catalysts

Catalyst	Conditions	Half-wave overpotential (η)	K_{obs} (s^{-1})	Ref.
$[Ni(P^{Ph}_2N^{C6H4X}_2)_2](BF_4)_2$	[4-$NCC_6H_4NH_3](BF_4)$; 0.12M (1.1M H_2O)	0.33 V	72	5
$[Ni(P^{R}_2N^{Ph}_2)_2(CH_3CN)](BF_4)_2$	$[(DMF)H]^+OTf^-$; H_2O, CH_3CN	0.45 V	69	6
$[Ni(7P^{Ph}_2N^{H})_2H]^{3+}$	Anilinium, CH_3CN	0.47 V	780	7
$\{[Ni_6(MeSi(^3py)_3)_8Cl_9(H_2O)_2]Cl_3\cdot16H_2O\}_\infty$	**0.017M acetic acid, CH_3CN**	**0.26 V**	**53**	**Present Work**

$P^{Ph}_2N^{C6H4X}_2$ = 1,5-di(*para*-X-phenyl); X= H; $P^{R}_2N^{Ph}_2$ = 1,5-diaza-3,7-diphosphacyclooctane; R= 2,4,4-trimethylpentyl; $7P^{Ph}_2N^{H}$ = 3,6-diphenyl-1-aza-3,6-diphosphacycloheptane

Table S5. Comparative photocatalytic HER activity of Ni(II) catalysts

Catalyst	PS & SR	Medium	TON	Longevity (h)	Ref.
$Ni(L)_2(H_2O)_2](BF_4)_2$	Fl & TEA	EtOH/H_2O at pH 10.5	3220	24	8
$[Ni(L')_3](BF_4)_2$;	Fl & TEA	EtOH/H_2O at pH 10.5	685	24	8
$Ni^{II}(L^{N_2Py_3})(MeCN)](ClO_4)_2$;	Fl & TEA	EtOH/H_2O at pH 12.0	3500	24	9
Nickel(II) phthalocyanine	$[Ir(dfppy)_2(dcbpy)$ & TEOA	CH_3CN/H_2O at pH 9.0	520	12	10
$(Et_4N)Ni(X\text{-}pyS)_3$	Fl & TEA	EtOH/ H_2O at pH 11.6	2282 ± 160	30	11
$Ni(mp)_2$	Fl & TEOA	H_2O at pH 9.8	5900	100	12
$Ni(mpo)_2$	CdSe & AA	H_2O at pH 4.5	308,000	128	12
$[Ni(P^{Ph}{}_2N^{Ph})_2](BF_4)_2$	$[Ru(bpy)_3]^{2+}$ & AA	CH_3CN / H_2O at pH 2.25	2700	150	13
$[Ni(P_2{}^{R'}N_2{}^{R''})_2]^{2+}$	RuP & AA	H_2O at pH 4.5	651± 30	30	14
$[Ni(P_2{}^{R'}N_2{}^{R''})_2]^{2+}$	CNx & EDTA	H_2O at pH 4.5	166.1 ± 20.6	3	15
$Ni_2(MBD)_4$	Fl & TEOA	CH_3CN / H_2O (v/v = 1:1) at pH 10.5	320	11	16
$Na_{28}[\{Ni_4(OH)_3AsO_4\}_4(\textit{B}\text{-}\alpha\text{-}PW_9O_{34})_4]\cdot 120H_2O$	$[Ir(ppy)_2(dtbbpy)]$ (PF_6) & TEOA	1.4 M H_2O in DMF/ CH_3CN	580	5	17
$Na4Li5[Ni_3(OH)_3(H_2O)_3P_2W_{16}$ $O_{59}]\cdot 48\ H_2O$	$[Ir(ppy)_2(dtbbpy)]$ (PF_6) & TEOA	H_2O/DMF/ CH_3CN (*v/v/v* =1:5:14)	160	3	18
$\{[Ni_6(MeSi(^3py)_3)_8Cl_9(H_2O)_2]$ $Cl_3\cdot 16H_2O\}_\infty$	**$[Ru(bpy)_3]^{+2}$ and AA**	**H_2O at pH 4.0**	**2824**	**69**	**Present work**

L=2-(2-pyridyl)-1,8-naphthyridine); L'=2-(2-pyridyl)quinoline); $L^{N_2Py_3}$=1,2-Benzenediamine, *N*^{1}-methyl-*N*^{1},*N*^{2},*N*^{2}-tris(2-pyridinylmethyl); X=CF_3; mp = 2-mercaptophenolate; mpo = 2- mercaptopyridyl-N-oxide; $P^{Ph}{}_2N^{Ph}$ = 1,3,6-triphenyl-1-aza-3,6diphosphacycloheptane; ($P_2{}^{R'}N_2{}^{R''}$)= bis(1,5-R′- diphospha-3,7-R″-diazacyclooctane), R'- Ph, R"- $PhCH_2P(O)(OH)_2$; MBD = 2-mercaptobenzimidazole; Fl= Fluorescein; TEA= Trietylamine, TEOA= Triethanolamine; AA= Ascorbic acid; RuP= Ru(II) tris(bipyridine); dfppy= 2-(2,4- difluorophenyl)-pyridine; dcbpy= 4,4'-dicarboxy-2,2' –bipyridine; CNx= polymeric carbon nitride; and bpy= 2,2'-Bipyridine.

References

1 M. S. Deshmukh, A. Yadav, R. Pant and R. Boomishankar, *Inorg. Chem.*, 2015, **54**, 1337–1345.

2 G. M. Sheldrick, *Acta Crystallogr. Sect. A Found. Crystallogr.*, 2008, **64**, 112–122.

3 A. M. Appel and M. L. Helm, *ACS Catal.*, 2014, **4**, 630–633.

4 G. A. N. Felton, R. S. Glass, D. L. Lichtenberger and D. H. Evans, *Inorg. Chem.*, 2006, **45**, 9181–9184.

5 U. J. Kilgore, J. A. S. Roberts, D. H. Pool, A. M. Appel, M. P. Stewart, M. R. DuBois, W. G. Dougherty, W. S. Kassel, R. M. Bullock and D. L. DuBois, *J. Am. Chem. Soc.*, 2011, **133**, 5861–5872.

6 U. J. Kilgore, M. P. Stewart, M. L. Helm, W. G. Dougherty, W. S. Kassel, M. R. DuBois, D. L. DuBois and R. M. Bullock, *Inorg. Chem.*, 2011, **50**, 10908–10918.

7 H. J. S. Brown, S. Wiese, J. A. S. Roberts, R. M. Bullock and M. L. Helm, *ACS Catal.*, 2015, **5**, 2116–2123.

8 P. Zhang, M. Wang, Y. Yang, D. Zheng, K. Han and L. Sun, *Chem. Commun.*, 2014, **50**, 14153–14156.

9 P. H. A. Kankanamalage, S. Mazumder, V. Tiwari, K. K. Kpogo, H. Bernhard Schlegel and C. N. Verani, *Chem. Commun.*, 2016, **52**, 13357–13360.

10 Y.-J. Yuan, J.-R. Tu, H.-W. Lu, Z.-T. Yu, X.-X. Fan and Z.-G. Zou, *Dalt. Trans.*, 2016, **45**, 1359–1363.

11 Z. Han, L. Shen, W. W. Brennessel, P. L. Holland and R. Eisenberg, *J. Am. Chem. Soc.*, 2013, **135**, 14659–14669.

12 A. Das, Z. Han, W. W. Brennessel, P. L. Holland and R. Eisenberg, *ACS Catal.*, 2015, **5**, 1397–1406.

13 P. Du and R. Eisenberg, *Energy Environ. Sci.*, 2012, **5**, 6012.

14 M. A. Gross, A. Reynal, J. R. Durrant and E. Reisner, *J. Am. Chem. Soc.*, 2014, **136**, 356–366.

15 C. A. Caputo, M. A. Gross, V. W. Lau, C. Cavazza, B. V. Lotsch and E. Reisner, *Angew. Chemie Int. Ed.*, 2014, **53**, 11538–11542.

16 H. Cui, J. Wang, M. Hu, C. Ma, H. Wen, X. Song and C. Chen, *Dalt. Trans.*, 2013, **42**, 8684.

17 H. Lv, Y. Chi, J. van Leusen, P. Kögerler, Z. Chen, J. Bacsa, Y. V. Geletii, W. Guo, T. Lian and C. L. Hill, *Chem. - A Eur. J.*, 2015, **21**, 17363–17370.

18 W. Guo, H. Lv, J. Bacsa, Y. Gao, J. S. Lee and C. L. Hill, *Inorg. Chem.*, 2016, **55**, 461–466